Predicting the Cocrystallization Behavior of Random Copolymers via Free Energy Calculations

Jürgen Wendling, Andrei A. Gusev, and Ulrich W. Suter*

Department of Materials, Institute of Polymers, ETH, CH-8092 Zürich, Switzerland

Received October 14, 1997; Revised Manuscript Received January 26, 1998

ABSTRACT: This contribution concerns the application of the thermodynamic-integration approach to crystalline structures. We calculate the defect Helmholtz energy of a single comonomer inclusion into the crystal structure of the host polymer via molecular-dynamics simulations. It was found that prior to the commonly applied scaling of the force field parameters, an additional scaling of some bond lengths and a modification of the short-distance nonbonded interaction potentials were necessary to avoid singularities and numerical instabilities during the free-energy calculations. The resulting defect Helmholtz energies for single inclusions in the system poly(ethylene terephthalate-*co*-2,6-dicarboxy naphthanoate) were considerably larger than the thermal energy and prohibit comonomer inclusion.

Introduction

Random copolymers are widely used as materials since they afford a convenient possibility of adjusting properties through the composition and constitution of the macromolecules. In the case of semicrystalline polymers, the degree of crystallinity in general decreases as the fraction of the minority comonomer increases, leading often to fully amorphous materials even at low concentrations of the comonomer. Only a few systems have been found where some crystallinity can be observed over the entire range of constitution. For those copolymers, a cocrystallization in either the crystal structure of the one or the other comonomer is observed.

It was shown by different authors,[1−5] that the probability P to find a comonomer (e.g., of type B) in a crystal of the host polymer of type A can be expressed by a "defect Gibbs energy", ϵ, which is the change in Gibbs energy of the crystal due to the incorporation of a B unit. For the case of thermodynamic equilibrium, this probability is given by the Boltzmann weight associated with ϵ, $P \propto \exp(-\epsilon/RT)$, and the concentration of comonomers B in the host crystal A then is[1]

$$X_{CB}(\text{eq}) = \frac{X_B e^{-\epsilon/RT}}{1 - X_B + X_B e^{-\epsilon/RT}} \qquad (1)$$

Here, we present an application of the computational method of thermodynamic integration to predict the Helmholtz energy of cocrystallization for random copolymer systems. We use the random copolymers of poly(ethylene terephthalate) (PET) and poly(ethylene naphthalene-2,6-dicarboxylate) (PEN), the cocrystallization behavior of PET−PEN random copolymers recently having been investigated by Lu and Windle.[6] Isodimorphism was observed with a change of the preferred crystal lattice type from PET-like to PEN-like at an over all concentration of ethylene-terephthalate in the copolymer of approximately 30 wt %. The chemical structures of these polymers are given in Figure 1.

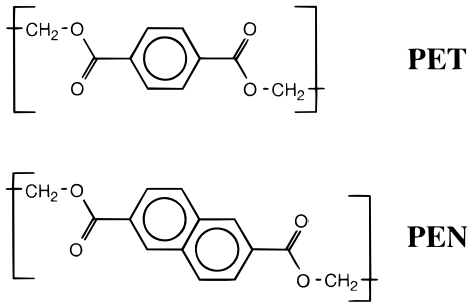

Figure 1. Chemical repeat units of poly(ethylene terephthalate) (PET) and poly(ethylene naphthalene-2,6-dicarboxylate) (PEN).

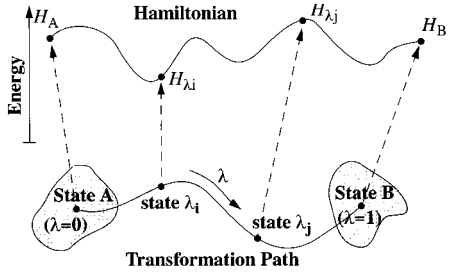

Figure 2. Scheme of the thermodynamic integration procedure.

Thermodynamic Integration

The computational method of thermodynamic integration is widely used for the prediction of free energy changes related to chemical modifications.[7] In general, this method describes the transformation of a given system from an initial state A, described by the Hamiltonian H_A, to a new state B (with Hamiltonian H_B) on an artificial transformation path (Figure 2). This path is described by a transformation coordinate λ that may run from 0 to 1 during the transformation and the related Hamiltonian H_λ is built up by a combination of H_A and H_B, i.e., $H_\lambda = f(1 - \lambda)\, H_A + f(\lambda)\, H_B$ where $f(\lambda)$ and $f(1 - \lambda)$ can be any continuously differentiable function of λ.

S0024-9297(97)01505-2 CCC: $15.00
Published on Web 03/31/1998

From the thermodynamic point of view, the Helmholtz energy difference $\Delta A_{BA} = A_B - A_A$ related to this transformation in an NVT ensemble is given by

$$\Delta A_{BA} = \int_A^B \left\langle \frac{\partial H(\lambda)}{\partial \lambda} \right\rangle_\lambda d\lambda \qquad (2)$$

To obtain this difference by molecular dynamics calculations, the Hamiltonian H (i.e., the underlying force field) has to be made λ-dependent and the thermodynamic average of $\partial H(\lambda)/\partial\lambda$ must be calculated for different values of λ to obtain a reliable approximation of the change in Helmholtz energy. Due to the additive character of the different terms in common force fields, all terms can have different dependencies on λ, with a physically totally unrealistic transformation path. One is free to choose a very smooth reaction path by an appropriate scaling of the different force-field terms, and the only considerations are convenience, accuracy, and computational efficiency. Here we present a scaling of force field parameters to calculate the Helmholtz energy difference for comonomer inclusions into a crystal structure of the host polymer.

As experimental results usually are obtained at constant pressure conditions, the calculated Helmholtz energy needs to be transformed into Gibbs energy for comparison. We approximate the Gibbs energy by subtracting the mean pressure energy $p\Delta V$ from the thermodynamic-integration results.

For all discussions on the terephthalate−naphthanoate transformation in this paper, a value of the coupling parameter of $\lambda = 0$ corresponds to the terephthalate structure whereas a value of $\lambda = 1$ corresponds to the naphthanoate structure. We consider the configuration at $\lambda = 0$ as the starting point of the thermodynamic integration and the configuration at $\lambda = 1$ as the finishing point. As the transformation is performed both in a PET and in a PEN crystal structure, this notation describes the creation of a naphthanoate defect in a PET host crystal or the annihilation of a terephthalate defect in a PEN host crystal. However, in the latter case the defect creation energy can be obtained by a simple change of the sign of all calculated derivatives.

Simulation Details

Molecular dynamics simulations were performed utilizing the Discover 95 molecular modeling package.[8] The PCFF91 force field[9] that is provided with this package was selected by comparing the average crystal unit cell dimensions of the polyesters under consideration to experimental results. It was found that the experimental values were matched within 5% in all cases. The nonbonded energy cutoff was set to 9.5 Å with a 1 Å spline function; a group-based cutoff was used to calculate Coulomb energies. During the molecular dynamics calculations, the temperature was kept fixed at 300 K using the Nosé−Hoover thermostat. If not explicitly indicated otherwise, the time step Δt of the molecular dynamics integration was set to 0.5 fs except for values of $\lambda \leq 0.1$ where 0.1 fs was applied. The sampling of conformations at a given value of λ was performed as follows: the equilibrium unit cell dimensions were taken as the average of a 50 ps NpT MD run on an appropriate crystal cell. Then, NVT MD runs for the sampling of an ensemble of representative crystal structures was started. At least the first 5 ps of this MD run were taken for further equilibration of the system; afterward, configurations were sampled with sampling intervals of 200 fs.

Derivatives $\partial H/\partial\lambda$ were calculated using a numerical differentiation approach. In particular, after sampling of conformations at a certain value of λ, we changed the force field so that it reflects a scaling parameter $\lambda' = \lambda + \delta$ or $\lambda' = \lambda - \delta$ and calculated the derivative as

$$\frac{\partial H}{\partial \lambda} = \frac{H(\lambda + \delta) - H(\lambda - \delta)}{2\delta} \qquad (3)$$

δ was set to a value of 0.01. Analytical derivatives were not used because of the complicated scaling of the force field that would make the analytical derivatives complex and time-consuming. The only exception are some components of the derivative at $\lambda = 0$ when the sampling of configurations was impossible. The analytical result (zero) was used for those components; see the following text for further details.

Numerical integration was performed applying the trapezoidal formula. The reported values include no estimate of the error induced by this integration approach since the results of physical relevance are differences between values calculated by the same method and a certain compensation of errors can be expected.

Thermodynamic averages were approximated by the mean values calculated on different conformations that were picked out of a molecular dynamics run. The snapshot frequency was 5 ps^{-1} for crystal structures and 1 ps^{-1} for single chains in a vacuum.

Statistical errors were estimated with the standard deviation σ of the sampled distribution of values and the number N of averaged values, $\sigma_{true} = \sigma/\sqrt{N}$. The blocking method as described by Flyvbjerg and Petersen[10] was used to ensure that the calculated statistical errors are not corrupted by correlation and it was found that the lower estimate of σ_{true} from this method is approximately $\sigma/\sqrt{N}$. This means that the correlation time of conformations that are sampled during a MD run is not longer than the sampling time step.

Scaling of the Force Field

From MD calculations on microstructures of the desired polyester crystals, we decided to employ the PCFF91 force field[9] because it fits well the experimental crystal lattice parameters of aromatic polyesters. In the scope of the present paper, the different scaling changes on the force field will be displayed on the model transformation of one terephthalate unit in a PET crystal microstructure into a naphthanoate unit, or vice versa.

During the thermodynamic-integration calculation, both "limiting structures" (i.e., naphthalene and benzene) are "interpolated" into an unrealistic structure containing both at different contributions, depending on λ. That means that "new" atoms and bonds have to be annihilated while other bonds are removed. Figure 3 sketches the transformation between units of PET and PEN. Notice that the PET repeat unit is obtained when the dark bonds are switched on ($\lambda = 0$), while the PEN repeat unit is obtained when the light bonds and atoms are active ($\lambda = 1$).

The number labels in the Figure are used for further reference. The letters denote the atom types of the

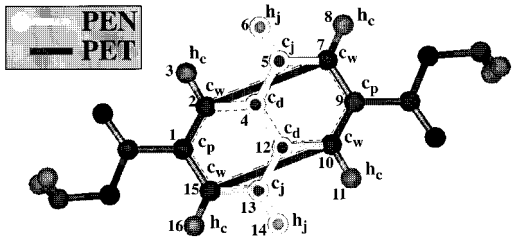

Figure 3. Combined terephthalate−naphthanoate repeat unit. See text.

PCFF91 force field: "c_p" and "h_c" are the common atom types for the carbon and hydrogen atoms of aromatic molecules such as benzene or naphthalene; "c_j," "c_d," "h_j" are similar atom types, having the same force-field parameters as "c_p" and "h_c" atoms for the PEN limiting structures ($\lambda = 1$); as these atoms are "created" during the thermodynamic-integration procedure, the parameters are scaled as described in the next paragraphs; atoms with atom type "c_w" are carbon atoms similar to "c_p", present in both limiting structures and with λ-invariant force field parameters (nevertheless, these special named atoms are necessary for the possibility of addressing bonds to atoms that are to be annihilated). In the following, the scaling functions for different types of interactions are discussed.

A. Internal Energies. In the PCFF91 force field, the different contributions to the internal energy are all linear functions of one or more force constants k. A linear scaling in λ of these force constants gives nonvanishing derivatives at $\lambda = 0$, difficult to evaluate numerically. Therefore, a scaling proportional to λ^2 is employed here, giving a contribution of the internal potential energy to the Hamiltonian H of

$$H_{\text{internal}}(\lambda) = \lambda^2 H_{\text{internal}}^{\text{unscaled}} \tag{4}$$

$H_{\text{internal}}^{\text{unscaled}}$ denotes the unscaled internal energy expression used in the original force field. This scaling leads to an analytic derivative of

$$\frac{\mathrm{d}H}{\mathrm{d}\lambda} = 2\lambda H_{\text{internal}}^{\text{unscaled}} \tag{5}$$

This λ^2 scaling was used for all internal energy contributions that were related to a newly created bond. The energy expression of bonds to be annihilated are similarly scaled with $(1 - \lambda)^2$. Energy contributions that would give direct interactions between both created and annihilated bonds (e.g., bending of the angle defined by $c_w-c_w-c_j$), were set to zero for all values of λ.

B. Bond Length Scaling. Bond stretching is the most sensitive contribution to the internal energy (with respect to the deformation from the equilibrium length) and controls the shape of the transforming molecule during the entire transformation. For example, the equilibrium bond length of two atoms having the force field atom type "c_w" is ca. 1.38 Å for the terephthalate unit but it would be ca. 3.66 Å for the naphthanoate unit (of course, $1 - \lambda = 0$ for the naphthanoate, and this "bond" does not contribute to the total potential energy). If the equilibrium bond length of this c_w-c_w bond were to remain constant at approximately 1.4 Å, the unit has to adapt a rooflike shape (rather than a flat one; see Figure 4) for a large λ range even when the force constants are drastically downscaled. Then, in a short part of the transformation path, the length

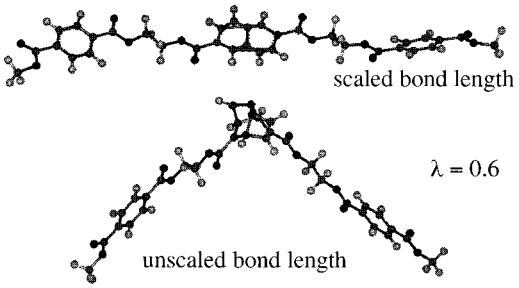

Figure 4. PET chain segment in vacuo, at 300 K, with one repeat unit under transformation to naphthanoate ($\lambda = 0.6$). Without scaling the bond length, a bend occurs at the position of the transformed unit. Scaling preserves the rigid shape of the segment.

Table 1. Equilibrium Bond Length Scaling for the Terephthalate−Naphthanoate Transition

bond	r_0 (λ)
c_w-c_w	$1.3823 + \lambda(3.6572 - 1.3823)$
c_w-c_j, c_j-c_d, c_d-c_w	$0.5225 + \lambda(1.3823 - 0.5225)$
c_d-c_d	$1.3823 + (1 - \lambda)\ 0.62944$

of these bonds would expand rather fast and the derivative of the bond length energy with respect to the scaling parameter λ would change dramatially, which makes the integration $\int_0^1 \langle \partial U(\lambda)/\partial\lambda \rangle\ \mathrm{d}\lambda$ very unreliable even when the interval $\Delta\lambda$ between two subsequent points of the trapezoidal integration procedure is small. To prevent this undesirable behavior, the c_w-c_w equilibrium bond length is also scaled linearly with λ; the other equilibrium bond lengths, i.e., c_w-c_j, c_j-c_d, c_d-c_w, and c_d-c_d were then derived from the c_w-c_w scaling by geometric arguments in such a way that the aromatic part remains approximately flat during the entire transformation. The final scaling functions are given in Table 1. Figure 4 gives some insight on the influence of this bond length scaling on the shape of a single chain with one repeat unit under transformation.

C. Intermolecular Nonbond Energies. The PCFF91 force field includes a 6−9 Lennard−Jones (LJ) van der Waals potential and Coulomb interactions. With the exception given below, we apply a λ^4 scaling to the force constants ϵ_u of the LJ potential leading to a λ^2 scaling of the interaction energy between one created and one unaffected atom (consider the mixing rule for the LJ pair interaction force constant $\epsilon_{uv} = 2(\epsilon_u\epsilon_v)^{1/2} f(r_u, r_v)$, where $f(r_u, r_v)$ is a function of the equilibrium radii r_u and r_v of atoms u and v). The partial charges created during the thermodynamic-integration simulation (on both atoms described by atom type h_j and both atoms typed c_w to which an h_j atom is connected) were subjected to a λ^2 scaling, leading to a Coulomb interaction energy with the same λ-dependence as the LJ interactions.

D. Intramolecular van der Waals and Coulomb Interactions. The bond length scaling discussed above enables transforming atoms to approach other atoms of the same monomer very closely. For example, one of the h_j atoms may easily reach the position of the c_w atom during an MD run, inducing singularities in $\mathrm{d}H_{\text{nonbond}}/\mathrm{d}\lambda$. For the intermolecular interactions, this problem does not occur because transforming atoms are covalently bonded to one chain and thereby are confined to positions reasonably far from atoms of one of the neighboring chains. To prevent singularities, we apply a smoothing function recently introduced by Beutler et

Table 2. List of Atom Pairs That Are Subjected to the Nonbonded Interaction Potential Given in Eqs 6 and 7

types of atom pairs	number in Figure 3
c_w-c_w	2−7, 10−15
c_w-c_p	1−7, 1−10, 2−9, 9−15
c_w-h_c	2−8, 3−7, 10−16, 11−15
c_w-h_j	2−6, 10−14

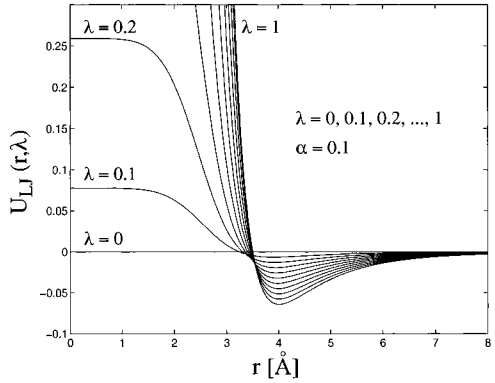

Figure 5. Modified Lennard−Jones potential (eq 6) for different values of λ.

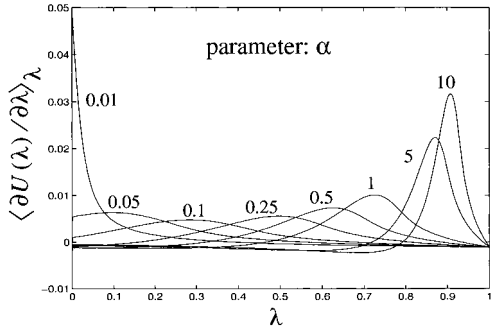

Figure 6. Derivative with respect to λ of the modified Lennard−Jones potential (eq 6) for different values of α.

al.[11] that is given here in a form translated to the 6−9 Lennard−Jones potential:

$$U_{LJ}(r,\lambda) = \frac{2\lambda\epsilon_{uv}}{(2\alpha(1-\lambda)^2 + (r_{uv}/\sigma_{uv})^6)^{9/6}} - \frac{3\lambda\epsilon_{uv}}{3\alpha(1-\lambda)^2 + (r_{uv}/\sigma_{uv})^6} \quad (6)$$

ϵ_{uv} and σ_{uv} are the potential well depth and the interatomic distance at which the minimum occurs; both are taken from the unscaled force field. α is a freely choosable parameter used to adjust the derivative $\partial U(\lambda)/\partial\lambda$ of this potential to a smooth function.

The atom pairs treated in this way are listed in Table 2. Also included in Table 2 are some atom pairs that are recognized as 1−2 or 1−3 interactions by the program's nonbonded interaction table setup (because the c_w-c_w bond always exists, even when this bond does not contribute to the potential energy at $\lambda = 1$) and that are, therefore, not automatically included into the nonbonded interaction table.

Figure 5 illustrates that the Lennard−Jones potential energy drops to zero for all distances r_{uv} in the limit $\lambda \rightarrow 0$. Figure 6 displays the dependence of the derivative $\langle \partial U(\lambda)/\partial\lambda \rangle_\lambda$ on λ (the simulated average was calculated applying a Boltzmann distribution on r_{uv}).

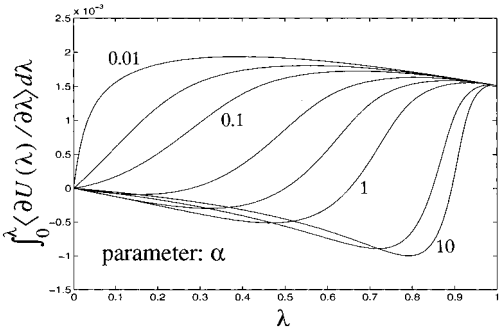

Figure 7. Convergence of the integral $\int_0^1 \langle \partial U(\lambda)/\partial\lambda \rangle \, d\lambda$ for the modified Lennard−Jones potential (Figure 6) and different values of α. See text for details.

We found a value of $\alpha = 0.1$ to be most suitable, since this yields the smoothest curve in Figure 6 and hence requires the fewest number of λ's during a thermodynamic integration run for a given final precision. The integral $\int_0^1 \langle \partial U(\lambda)/\partial\lambda \rangle \, d\lambda$ is not affected by this choice, as is demonstrated in Figure 7.

For Coulomb interactions, a similar interaction potential was applied:

$$U_{Coulomb}(\lambda) = \frac{\lambda q_u q_v}{4\pi D_0 D(\alpha(1-\lambda)^2 + r_{uv}^2)^{0.5}} \quad (7)$$

q_u and q_v are the partial charges of atoms u and v, r_{uv} is the interatomic distance, and D_0 and D are the permittivity of vacuum and the dielectric constant, respectively. Again, α was set to 0.1.

All these interaction energies and gradients were calculated in a home-built program written in C that runs in parallel to the Discover program and communicates via the Discover IPC interprocess communication port.[8]

E. Kinetic Energies. The atomic mass of atoms that are created during the thermodynamic integration calculation were scaled by a factor of λ^2. However, the mean kinetic contribution $H_{kinetic}$ to the total energy was constant at the equilibrium value of $^3/_2\ kT$ per atom, independent of λ.

Simulation of Crystalline Structures

If the exchange of a terephthalate unit for a naphthanoate unit is performed in a crystal structure subjected to periodic boundary conditions, care must be taken to consider finite size effects. Such a transformation in an oriented polyester chain changes the length of the chain by some angstroms, and models that contain "infinite" chains in one of the crystallographic directions can lead to unrealistic situations. We also found that "infinite" chains stabilize the shape of the simulation box and that the twist of the carbonyl group and the ethylene unit could be preserved only by keeping these "infinite" chains (across the cell boundaries). To access the effects of handling the problem of units of different lengths in a crystal, two different cases are considered.

Case 1. One Chain Becomes Longer. Analysis of some model structures revealed that the additional length contributed by the stiff aromatic unit can be accommodated to some extend by rearrangement of the flexible ethylene groups. Several repeat units away from the locus of transformation, along the chain, no significant shift of the atomic positions can be observed.

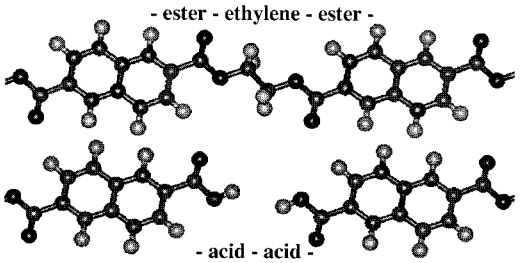

Figure 8. Modification of the polymer chain under transformation to allow relaxation.

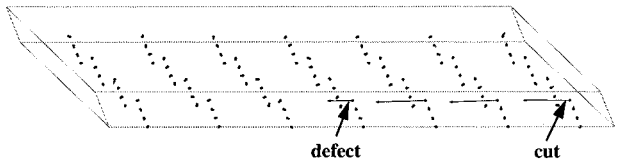

Figure 9. Displacements of PEN lattice sites (×3) after including one terephthalate unit and a cut in the same chain four repeat units away.

Therefore, a computational model that includes periodic boundary conditions in the direction of the polymer chain should be large enough so that the entire deformation "sphere" of a lattice defect can fit inside of the periodic model. Simulations on other chemical structures, not mentioned here, emphasize this conjecture. We conclude that only models with bonds across the cell boundaries are reliable and predictive.

Case 2. Shortening of a Chain. Contrary to the case where a unit was lengthened in the chain, here the defect chain is not able to "fix" the misfit in length by local bond rotation. A model with bonds across the cell boundaries ("infinite" chains) would distribute this misfit over the entire chain so that the defect were no longer localized. In reality, the chain would either relax by pulling more chains from the amorphous parts of the sample, or the defect would not be included into the crystal. The most plausible modeling approach seems to contain a "cut" in the chain where the defect was created, some repeat units away from the defect: the ester−ethylene−ester fragment is replaced here by two acid groups that are no longer covalently bonded to each other. To achieve this, we removed the C−C bond of the ethylene group, deleted the ethylene hydrogen atoms, and replaced the ethylene carbon atoms by hydrogen atoms (see Figure 8). The partial charge of the acid oxygen was kept at the value (−0.1163) of the ester group oxygen in polymers and the charge of the new hydrogen atom was set to 0.1133 to achieve electron neutrality of the model. In this way, the chain length is able to relax during the thermodynamic integration calculation.

Figure 9 displays the deformation vectors of a PEN model including 4 × 4 chains with 7 repeat units each, where in one chain one naphthalene unit was replaced by a benzene ring and a cut was introduced as described above. Observe that one "end" of this chains essentially remains at the original position whereas the other end slips to relax the structure.

The Helmholtz Energy Change of Comonomer Inclusion

Consider the inclusion of a single copolymer repeat unit into the crystal structure of the host polymer. We will focus on the copolymer system PET−PEN and discuss both the inclusion of a shorter repeat unit (i.e., a benzene instead of a naphthalene in a PEN crystal) and of a longer repeat unit (a naphthalene instead of benzene in a PET crystal). A number of "experiments", not reported here, has shown that the "chemical transformation" between the units of interest here, i.e., between benzene and naphthalene, is not well-described by thermodynamic integration with the force field at hand.[12] This is not surprising, given the electronically delocalized nature of these moieties and the oversimplified and highly localized description of the force field. As we are not interested in the free energy change of a chemical transformation but only in the defect free energy upon inclusion of the transformed unit into a crystal, care must be taken to analyze which part of the transformation free energy contributes to the defect free energy and which does not. We define the noncontributing parts as the reference state.

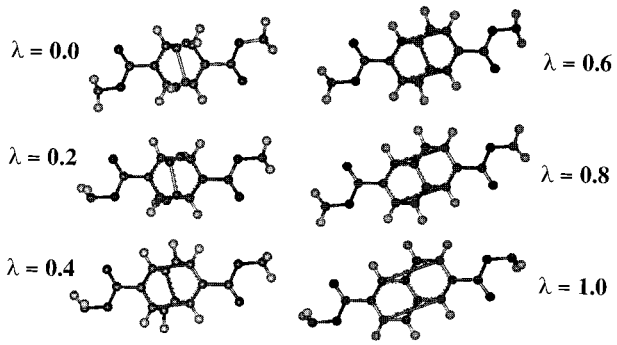

Figure 10. Snapshots of the repeat unit under transformation taken from MD calculations on short polymer chains.

A. The Reference State. The transformation of one polymer sequence, embedded in a crystal, into another one can be divided into two parts: a free energy change that reflects only the chemical permutation without introducing any interactions to the neighboring crystal unit cells and a free energy change that describes the cohesive stability of the crystal and packing constraints. The latter fully belongs to the defect free energy; the reference state must be free from any external constraints and also from nonbonded interactions, except for those which are intramolecular.

Therefore, a suitable model for the reference state is a short, noncoiled single chain. We used a fragment that contains three repeat units, the central one under transformation. The applied nonbonded interaction cutoff distance was shorter than the repeat unit length of the polyesters under consideration, and the results therefore do not depend on the chemical structure of the aromatic unit of the first and third repeat unit (i.e., whether it is benzene or naphthalene). However, we performed two independent calculations with different chemical structures (either the first and third units were both terephthalate or were both naphthanoate) in order to estimate the errors occurring in the thermodynamic-integration procedure on independent runs. The noncoiled conformation was preserved by constraining the end-to-end distance between 25 and 40 Å, applying a flat bottomed potential.

Values of $\langle \partial H(\lambda)/\partial\lambda \rangle_\lambda$ on single chains were calculated from MD runs of 500 ps for each value of λ. Snapshots were taken every 1 ps to calculate the derivative. Figure 10 gives the shapes of arbitrarily selected snapshots of the repeat unit under transformation for different values of λ. It is obvious that almost no

Table 3. Mean Values and Statistical Deviations of $\langle \partial H(\lambda)/(\partial\lambda)\rangle_\lambda$ for the Transformation from Terephthalate to Naphthanoate in Both Isolated PET and Isolated PEN Chain Segments (Values in kJ/mol)

	transformation terephthalate → 2,6-dicarboxy naphthanoate			
	in a PET chain segment		in a PEN chain segment	
λ	$\langle \partial H(\lambda)/\partial\lambda\rangle_\lambda$	stat dev	$\langle \partial H(\lambda)/\partial\lambda\rangle_\lambda$	stat dev
0.0	−69	16	−104	16
0.1	576	17	563	17
0.2	594	14	602	14
0.4	555	11	523	10
0.6	388	8	390	8
0.8	539	8	526	8
0.9	654	9	642	8
1.0	605	11	639	11

Table 4. Helmholtz Energy Changes (kJ/mol) Calculated for the Transformation Terephthalate−2,6-Dicarboxy Naphthanoate in Two Independent Calculations

transformation terephthalate−naphthanoate	$\Delta A = \int \langle \partial H(\lambda)/\partial\lambda\rangle_\lambda \, d\lambda$
in a PET chain segment	508 ± 11
in a PEN chain segment	500 ± 10
mean value	504 ± 10

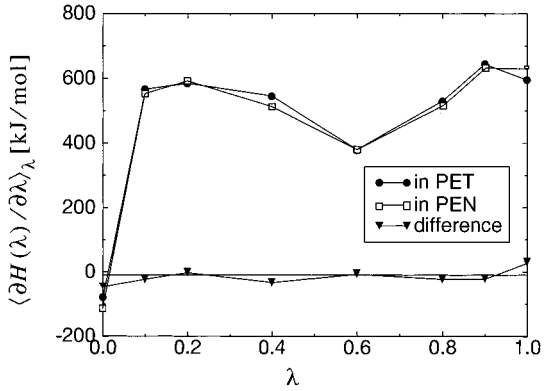

Figure 11. Mean values of $\langle \partial U(\lambda)/\partial\lambda\rangle_\lambda$ for the transformation of a terephthalate into a 2,6-dicarboxy naphthanoate unit in isolated PET and PEN chains.

deformation of the flat habit of the aromatic unit occurs during the transformation, due to the scaling of several bond length (see above). Table 3 lists the results of the runs.

The calculated derivatives are similar for both calculations and the difference is in the range of the statistical deviations. Figure 11 points out that the deviations compensate over the range of λ.

The integration of $\langle \partial H(\lambda)/\partial\lambda\rangle_\lambda$ according to eq 2 and the use of the trapezoidal integration rule give the free energy values reported in Table 4. We defined the mean value of 503.8 kJ/mol as the reference value of this type of transformation. Its precision is not better than approximately 11 kJ/mol.

B. Crystal Defect Calculations. Following the procedure indicated above in the section "Simulation Details," thermodynamic integration calculations were carried out on crystal microstructures of 16 or 24 chains with 7 repeat units each. The mean values $\langle \partial H(\lambda)/\partial\lambda\rangle_\lambda$, obtained on 150 frames taken every 200 fs during a 30 ps MD run, after 5 ps of equilibration, are given in Table 5 and Figure 12. Figure 13 addresses the convergence of these derivatives.

On the basis of these results, the integration of $\langle \partial H(\lambda)/\partial\lambda\rangle_\lambda$ with respect to λ was performed using the trapezoidal scheme. The results of this thermodynamic integration calculation is given in Table 6. In the last columns, we subtracted the reference value of 503.8 kJ/mol to obtain the defect Helmholtz and Gibbs energy of a single comonomer inclusion.

These values are very high compared to the thermal energy (RT is 2.49 kJ/mol), so no inclusion of comonomer defects can be expected in the PET/PEN system. An assessment of the values obtained will be made in the companion paper.[14]

Table 5. Mean Values and Statistical Deviations of $\langle \partial H(\lambda)/(\partial\lambda)\rangle_\lambda$ for the Creation of One Terephthalate Defect in a PEN Crystal and One Naphthanoate Defect in a PET Crystal (Values in kJ/mol)

	naphthanoate in a PET crystal		terephthalate in a PEN crystal	
λ	$\langle \partial H(\lambda)/\partial\lambda\rangle_\lambda$	stat dev	$\langle \partial H(\lambda)/\partial\lambda\rangle_\lambda$	stat dev
0.0	−73	30	78	32
0.1	628	28	−662	32
0.2	639	24	−447	23
0.4	600	19	−310	18
0.6	562	17	−298	15
0.8	641	14	−477	15
0.9	741	18	−568	17
1.0	744	20	−616	18

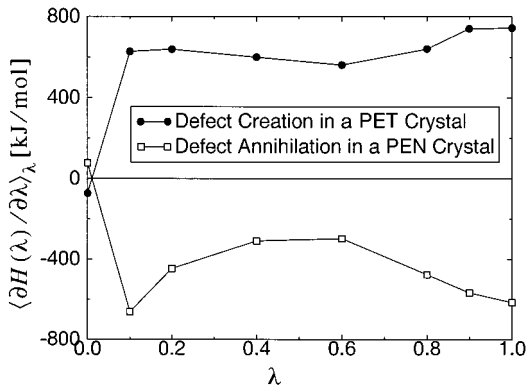

Figure 12. Graphical representation of values given in Table 5.

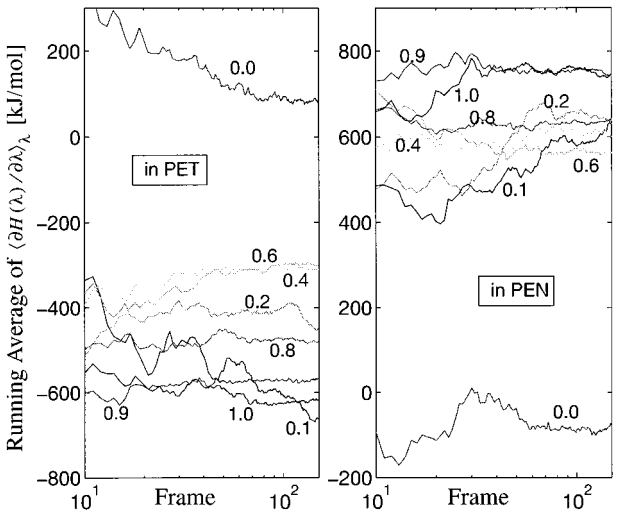

Figure 13. Converging of the derivative for the transition terephthalate−2,6-dicarboxy naphthanoate in a PET crystal and in a PEN crystal.

The Necessity of Gibbs Energy Calculations

The reader may ask why we treat our problem using this highly elaborated method instead of simple defect

Table 6. Values of the Helmholtz Energy Change Calculated for the Inclusion of a 2,6-Dicarboxy Naphthanoate Defect into a PET Crystal and of a Terephthalate Defect into a PEN Crystal[a]

transformation	ΔA (kJ/mol)	defect energy (kJ/mol) Helmholtz	Gibbs
naphthanoate in a PET crystal	595 ± 20	91 ± 23	86 ± 23
terephthalate in a PEN crystal	-414 ± 20	90 ± 23	85 ± 23

[a] The defect Helmholtz energy was obtained by substracting the reference energy given in Table 4. Defect Gibbs energy is obtained after correcting for the mean pressure energy, $p\Delta V$.

energy calculations. Indeed, the difference in total energy, taken from 30 ps NVT MD calculations at $\lambda = 0$ and $\lambda = 1$, after inclusion of one naphthanoate unit into the PET crystal is 569 kJ/mol, close to the Helmholtz energy difference of 595 kJ/mol. Subtracting the total energy change from the single chain calculations, a defect total energy difference of 76 kJ/mol remains. Therefore, the comparatively small entropic contribution to the defect Helmholtz energy of $T\Delta S \approx 15$ kJ/mol does not change our interpretation.

In general, however, entropy can play as large a role as enthalpy (or larger) in the inclusion defect free energy. A case where the entropic contributions are as significant as those from enthalpy changes can be found when considering the inclusion of many defects (not shown here). In that case, the average defect energy should decrease by favorable aggregation of comonomers. As an example, we exchanged a complete a−b naphthanoate layer of a PEN microstructure (24 chains of five repeat units each) by terephthalate units. Thermodynamic integration calculations were performed in an NpT ensemble for 10 ps per λ value. The variation of the microstructure cell parameters shows that the transformation is continuous, making the thermodynamic integration possible. The average defect Gibbs energy was obtained to 21 ± 7 kJ/mol, composed of a total energy difference of 51 kJ/mol and an entropic contribution of $T\Delta S = 30 \pm 7$ kJ/mol. Although this result is considerably larger than RT, making equilibrium inclusion rather unlikely, nonequilibrium inclusion (i.e., a crystal defect concentration higher than that given by eq 1) could occur. Another case, where the inclusion of a single defect is actually dominated by the entropy contributions, is the system poly(β-hydroxybutyrate-*co*-β-hydroxyvalerate), which will be described in detail in a separate publication.[15]

Acknowledgment. We gratefully acknowledge financial support from the DSM and Akzo Nobel (The Netherlands) and for J.W. from the Deutsche Forschungsgemeinschaft (Grant No. DFG We 2134/1-1). We also appreciate stimulating discussions with Luc Leemans, Rob Meier, Ad Braam (DSM), Jos Aerts, Marcel Hottenhuis and Jurriaan v.d. Heuvel (Akzo Nobel) and Birgitta Nick and Serge Santos of the Department of Materials at ETH.

References and Notes

(1) Sanchez, I. C.; Eby, R. K. *Macromolecules* **1975**, *8*, 638.
(2) Allegra, G.; Marchessault, R. H.; Bloembergen, S. *J. Polym. Sci., Part B: Polym. Phys.* **1992**, *30*, 809.
(3) Goldbeck-Wood, G. *Polymer* **1992**, *33*, 778.
(4) Orts, W. J.; Marchessault, R. H.; Bluhm, T. L. *Macromolecules* **1991**, *24*, 6435.
(5) Kamiya, N.; Sakurai, M.; Inoue, Y.; Chujo, R. *Macromolecules* **1991**, *24*, 3888.
(6) Lu, X.; Windle, A. H. *Polymer* **1995**, *36*, 451.
(7) van Gunsteren, W. F.; Beutler, T. C.; Fraternali, F.; King, P. M.; Mark, A. E.; Smith, P. E. In *Computer Simulations of Biomolecular Systems: Theoretical and Experimental Applications*, van Gunsteren, W. F., Weiner, P. K., Wilkinson, A. J., Eds.; ESCOM: Leiden, Eds.; 1993.
(8) InsightII and Discover 95. MSI Molecular Simulations, San Diego, CA, 1995.
(9) Hwang, M. J.; Stockfisch, T. P.; Hagler, A. T. *J. Am. Chem. Soc.* **1994**, *116*, 2515.
(10) Flyvbjerg, H.; Petersen, H. G. *J. Chem. Phys.* **1989**, *91*, 461.
(11) Beutler, T. C.; Mark, A. E.; van Schaik, R. C.; Gerber, P. R.; van Gunsteren, W. F. *Chem. Phys. Lett.* **1994**, *222*, 529.
(12) Mordasini Denti, T. Z.; Beutler, T. C.; van Gunsteren, W. F.; Diederich, F. *J. Phys. Chem.* **1996**, *100*, 4256.
(13) Mencik, Z. *Chemicky Prumysl* **1967**, *42*, 78.
(14) Wendling, J.; Suter, U. W. *Macromolecules* **1998**, *31*, 2516.
(15) Wendling, J.; Suter, U. W. Manuscript in preparation.

MA971505L